SHAW, PITTMAN, POTTS & TROWBRIDGE

A PARTNERSHIP INCLUDING PROFESSIONAL CORPORATIONS

1800 M STREET, N. W.
WASHINGTON, D. C. 20036
(202) 822-1000

TELECOPIER
(202) 822-1099 & 822-1199

RAPIFAX 100
(202) 822-1072

TELEX
89-2693 (SHAWLAW WSH)
CABLE "SHAWLAW"

VIRGINIA OFFICE
1501 FARM CREDIT DRIVE
MCLEAN, VIRGINIA 22102
(703) 790-7900

TELECOPIER
(703) 821-2397

February 28, 1986

WRITER'S DIRECT DIAL NUMBER
822-1474

Morton B. Margulies, Chairman
Atomic Safety and Licensing
Board
U.S. Nuclear Regulatory
Commission
Washington, D.C. 20555

Mr. Gustave A. Linenberger, Jr.
Atomic Safety and Licensing
Board
U.S. Nuclear Regulatory
Commission
Washington, D.C. 20555

Dr. Oscar H. Paris
Atomic Safety and Licensing
Board
U.S. Nuclear Regulatory
Commission
Washington, D.C. 20555

In the Matter of
Georgia Power Company, et al.
(Vogtle Electric Generating Plant, Units 1 and 2
Docket Nos. 50-424 and 50-425OL

Gentlemen:

Attached for the information of the Licensing Board and of the parties is a draft report, "Ground-water Numerical Modeling" (February 1986).

Sincerely,

David R. Lewis
Counsel for Applicants

cc w/encl:
Service List

DS03

UNITED STATES OF AMERICA
NUCLEAR REGULATORY COMMISSION

Before the Atomic Safety and Licensing Board

In the Matter of	)	
	)	
GEORGIA POWER COMPANY, et al.	)	Docket No. 50-424
	)	50-425
(Vogtle Electric Generating Plant,	)	
Units 1 and 2)	)	

SERVICE LIST

Morton B. Margulies, Chairman
Atomic Safety and Licensing Board
U.S. Nuclear Regulatory Commission
Washington, D.C. 20555

Mr. Gustave A. Linenberger
Atomic Safety and Licensing Board
U.S. Nuclear Regulatory Commission
Washington, D.C. 20555

Dr. Oscar H. Paris
Atomic Safety and Licensing Board
U.S. Nuclear Regulatory Commission
Washington, D.C. 20555

Bernard M. Bordenick, Esq.
Office of Executive Legal Director
U.S. Nuclear Regulatory Commission
Washington, D.C. 20555

Bradley Jones, Esquire
Regional Counsel
U.S. Nuclear Regulatory Commission
Suite 3100
101 Marietta Street
Atlanta, GA 30303

Atomic Safety and Licensing Board Panel
U.S. Nuclear Regulatory Commission
Washington, D.C. 20555

Atomic Safety and Licensing Appeal Board Panel
U.S. Nuclear Regulatory Commission
Washington, D.C. 20555

Douglas C. Teper
1253 Lenox Circle
Atlanta, Georgia 30306

Tim Johnson
Campaign for a Prosperous Georgia
1083 Austin Avenue, N.E.
Atlanta, GA 30307

Docketing and Service Section
Office of the Secretary
U.S. Nuclear Regulatory Commission
Washington, D.C. 20555

DRAFT

VOGTLE ELECTRICAL GENERATING PLANT

GROUND-WATER NUMERICAL MODEL

Bechtel Inc.

February 1986

GROUND-WATER NUMERICAL MODEL FOR VOGTLE

A numerical model was used to simulate the ground-water conditions at the Vogtle plant site and its vicinity. It was intended to complement the analytical calculations of ground-water flow and travel times. The specific objectives of the ground-water flow simulation for the Vogtle site were to:

1. Investigate if the assumption of persistently high permeabilities of Utley limestone throughout the area is consistent with water levels in the vicinity of the site;

2. Determine the location of the ground-water divide with respect to the power-block area; and

3. Investigate the influence of backfill on water levels in the power block area.

The methodology and results of the numerical analysis and the conclusions derived therefrom are described in the following sections. The numerical model used is GS2, described in "Documentation and User's Guide: GS2 & GS3 - Variably Saturated Flow and Mass Transport Models" (NUREG/CR-3901, April 1985).

I. Ground-Water Flow Simulation

The finite-element mesh used for the ground-water flow simulation is shown in Figure 1. This mesh contains 455 nodes and 413 elements. To improve accuracy, the mesh is refined in the power block area where the nodal spacing is approximately equal to 150 ft. The elements become progressively larger toward the boundaries.

The boundary conditions imposed on the model are shown in Figure 1. The model extends to the streams bordering the interfluvial ridge on which the plant is located. The boundary conditions of the model at these streams are constant head conditions. That is, water levels remain at the elevation of the streams at these boundaries, or, as in the case of the boundary along the Savannah River, at the top of the marl exposed along the bluff. The levels of the streams were determined from the U.S. Geological Survey 7.5-minute quadrangle topographic sheets covering the area. The top of the marl was taken from Figure 2.5.1-30 of the Vogtle FSAR. Beneath the narrow area at the northwest boundary between the Mathes Pond drainage and the tributary to Daniels Branch, no-flow conditions are specified.

An average annual recharge rate equal to 15 inches was specified throughout the model. This is a maximum of reported values for the region and corresponds to about one third of the average annual precipitation in the area.

The transmissivity in the study area, based on field and laboratory tests, is postulated to range from 2,000 to 25,000 gpd/ft (gallons per day per foot) in the north where the Utley limestone is present, and between 500 and 4,000 gpd/ft in the south where only the sands of the

Barnwell Group are present. Transmissivity values within these ranges were successively assumed in the model until a satisfactory agreement between calculated and observed water levels prior to construction was obtained. The water-level data prior to construction were used for calibration of the model because they most closely approximate a steady-state condition. The results of this calibration procedure are presented below.

The water levels used as a reference for the model calibration were weighted averages of measurements made between January 1, 1971, and May 30, 1974, at each of thirteen wells located at the site of the Vogtle plant prior to construction. It is assumed that the reported water levels taken during that period are all valid measurements representing the water table. Because there are few observation wells in the southern part of the study area, the local topography was used to provide upper bounds to the model results. Specifically, criteria for acceptable results in the southern part of the study area are that water levels cannot be higher than a level 20 feet below ground surface.

II. Model Test Cases

The T (transmissivity) distribution that was found to provide the most satisfactory agreement between measured and calculated water levels is shown in Figure 2. This simulation assumes three areas of aquifer materials with similar T values equal to, from north to south, 16,000 gpd/ft (area 1), 8,000 gpd/ft (area 4), and 2,000 gpd/ft (area 2). The Utley limestone is present in areas 1 and 4. The results of the simulation are shown in Figures 3A and 3B, and in Table 1. Area 3, not included in this simulation, is the area excavated to the marl and backfilled for the power block structures. It is the rectangular area within the dashed line of Figure 3B. Figure 3A presents five-foot contours of the calculated water levels for this combination of transmissivity and a recharge rate of 15 in/yr. Figure 3B is a close-up view of the power block area, with one-foot contour intervals. The weighted-average water level measurements are shown in parentheses next to the well locations in the figures.

Figures 4 through 8 present results assuming different distributions of transmissivity in the study area. Figures 4A and 4B and Table 2 show the results obtained with T = 16,000 gpd/ft in areas 1 and 4 and T = 2,000 gpd/ft in area 2; the same combination of transmissivities as in Figures 3A and 3B except that the transmissivity in area 4 is increased to 16,000 gpd/ft (equal to that of area 1). The results of this case is similar to that of Figures 3A and 3B. However, the fit to the south of the power block (i.e.; well 124) is not as satisfactory as when the intermediate transmissivity zone is included in the model (compare Tables 1 and 2).

In Figures 5A and 5B, T is increased to 20,000 gpd/ft in areas 1 and 4, and T in area 2 is decreased to 400 gpd/ft. This combination of transmissivities is seen to yield water levels that are too low in the north and excessively high in the south (Table 3), and is considered unsatisfactory.

Figures 6A and 6B, and Table 4 correspond to the case when T = 16,000 gpd/ft in area 1, 8,000 gpd/ft in area 4, and 4,000 gpd/ft in area 2; that is, same conditions as in Figures 3A and 3B and Table 1, except that the transmissivity in the southern part of the model has been increased.

Figures 7A and 7B (Table 5), and Figures 8A and 8B (Table 6) are two additional cases applying T = 8,000 gpd/ft in area 4 and 4,000 gpd/ft in area 2, but reducing the transmissivity in the northern part of the model, (area 1); first to 12,000 gpd/ft and then to 8,000 gpd/ft, respectively. Neither of these cases are found to improve the model calibration achieved in Figure 3, which is therefore considered the best case among the simulations performed in this study to fit the apparent weighted average water-level conditions prior to construction.

III. <u>Influence of Backfill on Water Levels</u>

Figures 9A and 9B and Table 7 show the results when backfill material is included in the model at the power block excavation. The backfill material was assigned a transmissivity of 8[illegible]0 gpd/ft (area 3) based on a permeability of 1200 ft/yr and a thickness of 35 feet. The zone of backfill material is that area inside the dashed rectangle on Figures 9A and 9B. Recharge in the model is assumed to be similar to preconstruction conditions except in the power block excavation area. In that area it is restricted to the portion that will not be covered by surface paving or buildings. The largest open area available to recharge is in the southern portion of the backfill. The calculated water levels in the power-block area with backfill in-place are slightly higher than without backfill (i.e., Figures 3A and 3B).

IV. <u>Conclusions</u>

Based on the results of the numerical modeling presented in Sections II and III it is concluded that:

1. Of the model test cases used in this study, the closest approximation of transmissivities in the study area is as shown in Figure 2, wherein the study area is divided into three transmissivity zones: 16,000 gpd/ft in the northern part (area 1), 2,000 gpd/ft in the southern part (area 2), and 8000 gpd/ft in a transition zone (area 4) between the high- and low-transmissivity regions.

2. High permeabilities (i.e., transmissivities greater than 16,000 gpd/ft) are not persistent in the area underlain by the Utley limestone.

3. Over the range of transmissivity values modeled, the ground-water divide remains south of the plant.

4. A slight rise in water levels is apparent beneath the power block area when the backfill material is considered. The direction of ground-water flow remains from south to north beneath the power block.

Table 1 - Match of Water Levels at Wells by "Best-Fit" Case

Observation Wells		Model Simulation	
No.	Water Level Elev. (Weighted Average, Ft)	Water Elev. (Ft)	Difference (Ft)
42D	159	161	2
124	166	166	0
129	158	160	2
140	164	160	-4
142	156	157	1
143	158	159	1
176	164	165	1
177	164	160	-4
178	161	160	-1
243	148	156	8
244	160	158	-2
245	160	161	1
249	163	160	-3

Statistics of water level differences:

Arithmetic mean	0.2
Standard deviation	3.1
Sum of squares divided by N (N=13)	9.4

Table 2 - Match of Water Levels at Wells by Test Case 1

Observation Wells		Model Simulation	
No.	Water Level Elev. (Weighted Average, Ft)	Water Elev. (Ft)	Difference (Ft)
42D	159	162	3
124	166	165	-1
129	158	161	3
140	164	161	-3
142	156	157	1
143	158	160	2
176	164	165	1
177	164	162	-2
178	161	160	-1
243	148	156	8
244	160	159	-1
245	160	162	2
249	163	161	-2

Statistics of water level differences:

Arithmetic mean	0.8
Standard deviation	2.8
Sum of squares divided by N (N=13)	8.6

Table 3 - Match of Water Levels at Wells by Test Case 2

Observation Wells		Model Simulation	
No.	Water Level Elev. (Weighted Average, Ft)	Water Elev. (Ft)	Difference (Ft)
42D	159	165	6
124	166	169	3
129	158	163	5
140	164	164	0
142	156	160	4
143	158	162	4
176	164	174	10
177	164	166	2
178	161	160	-1
243	148	158	10
244	160	161	1
245	160	165	5
249	163	164	1

Statistics of water level differences:

Arithmetic mean	3.8
Standard deviation	3.3
Sum of squares divided by N (N=13)	25.7

Table 4 - Match of Water Levels at Wells by Test Case 3

Observation Wells		Model Simulation	
No.	Water Level Elev. (Weighted Average, Ft)	Water Elev. (Ft)	Difference (Ft)
42D	159	158	-1
124	166	161	-5
129	158	158	0
140	164	158	-6
142	156	155	-1
143	158	157	-1
176	164	159	-5
177	164	157	-7
178	161	160	-1
243	148	154	6
244	160	156	-4
245	160	158	-2
249	163	158	-5

Statistics of water level differences:

Arithmetic mean	-2.5
Standard deviation	3.3
Sum of squares divided by N (N=13)	16.9

Table 5 - Match of Water Levels at Wells by Test Case 4

Observation Wells		Model Simulation	
No.	Water Level Elev. (Weighted Average, Ft)	Water Elev. (Ft)	Difference (Ft)
42D	159	160	1
124	166	162	-4
129	158	159	1
140	164	159	-5
142	156	156	0
143	158	159	1
176	164	160	-4
177	164	158	-6
178	161	160	-1
243	148	156	8
244	160	158	-2
245	160	160	0
249	163	159	-4

Statistics of water level differences:

Arithmetic mean	-1.2
Standard deviation	3.5
Sum of squares divided by N (N=13)	13.9

Table 6 - Match of Water Levels at Wells by Test Case 5

Observation Wells		Model Simulation	
No.	Water Level Elev. (Weighted Average, Ft)	Water Elev. (Ft)	Difference (Ft)
42D	159	165	6
124	166	167	1
129	158	164	6
140	164	164	0
142	156	161	5
143	158	163	5
176	164	164	0
177	164	163	-1
178	161	161	0
243	148	160	12
244	160	162	2
245	160	164	4
249	163	163	0

Statistics of water level differences:

Arithmetic mean	3.1
Standard deviation	3.6
Sum of squares divided by N (N=13)	22.2

Table 7 - Match of Water Levels at Wells by Test Case 6

Observation Wells		Model Simulation	
No.	Water Level Elev. (Weighted Average, Ft)	Water Elev. (Ft)	Difference (Ft)
42D	159	159	0
124	166	166	0
129	158	159	1
140	164	160	-4
142	156	157	1
143	158	158	0
176	164	166	2
177	164	160	-4
178	161	160	-1
243	148	155	7
244	160	157	-3
245	160	160	0
249	163	159	-4

Statistics of water level differences:

Arithmetic mean	-0.4
Standard deviation	2.9
Sum of squares divided by N (N=13)	8.7

Figure 1 - Vogtle GS2 Finite Element Mesh With Boundary Conditions

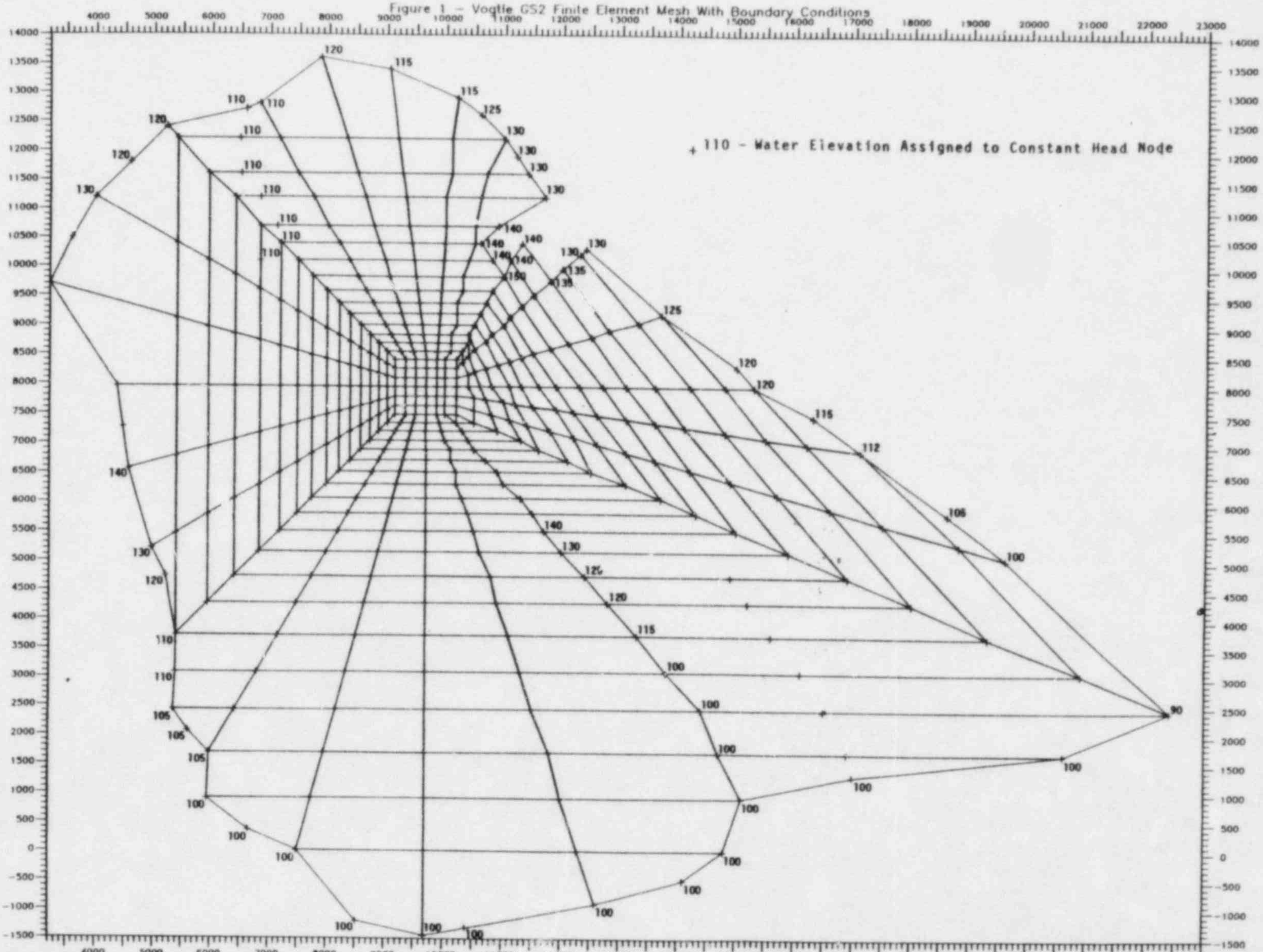

Figure 2 – Vogtle GS2 Material Transmissivities for Best-Fit Case

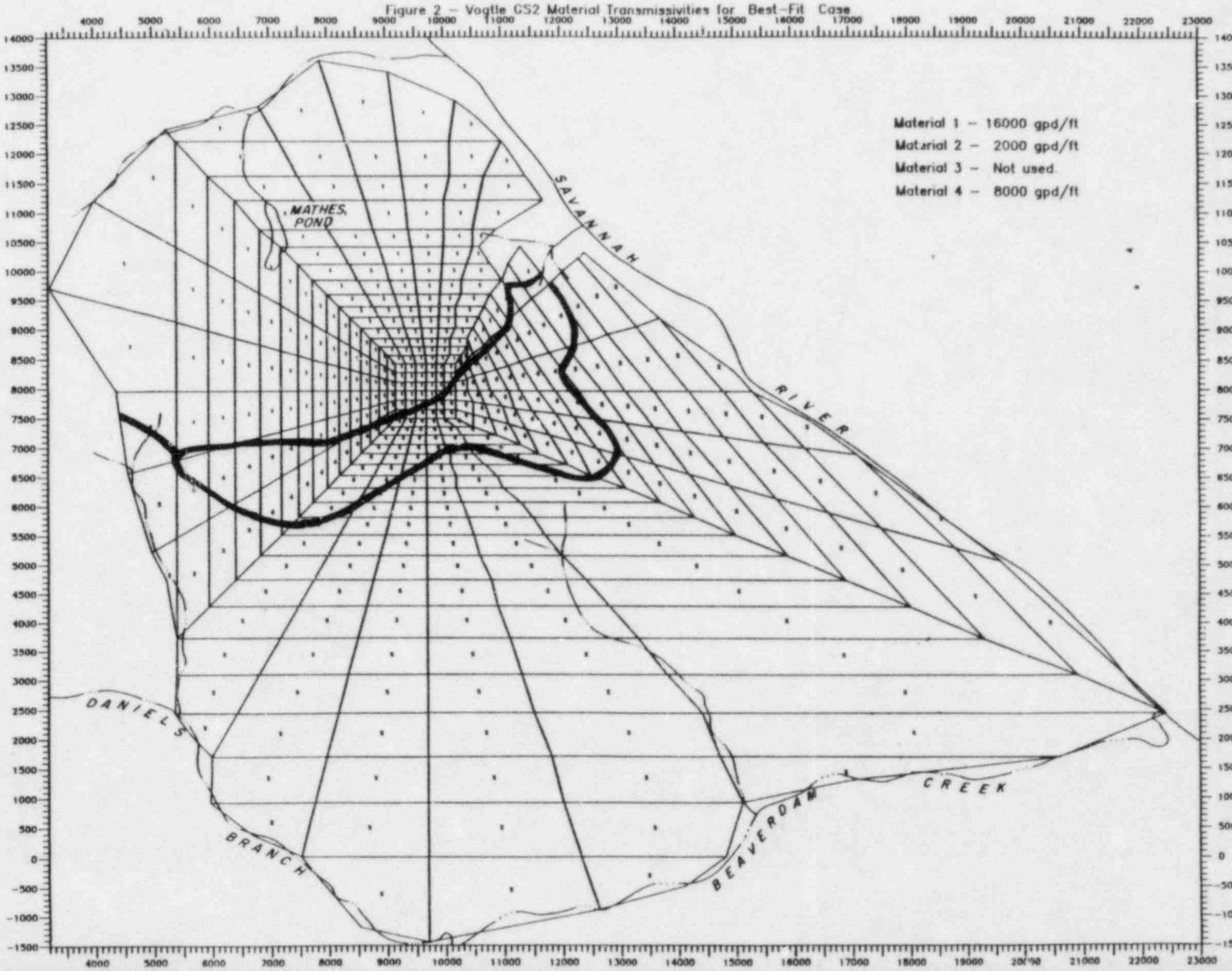

Figure 3A – Vogtle GS2 Water-Table Contours for Best-Fit Case

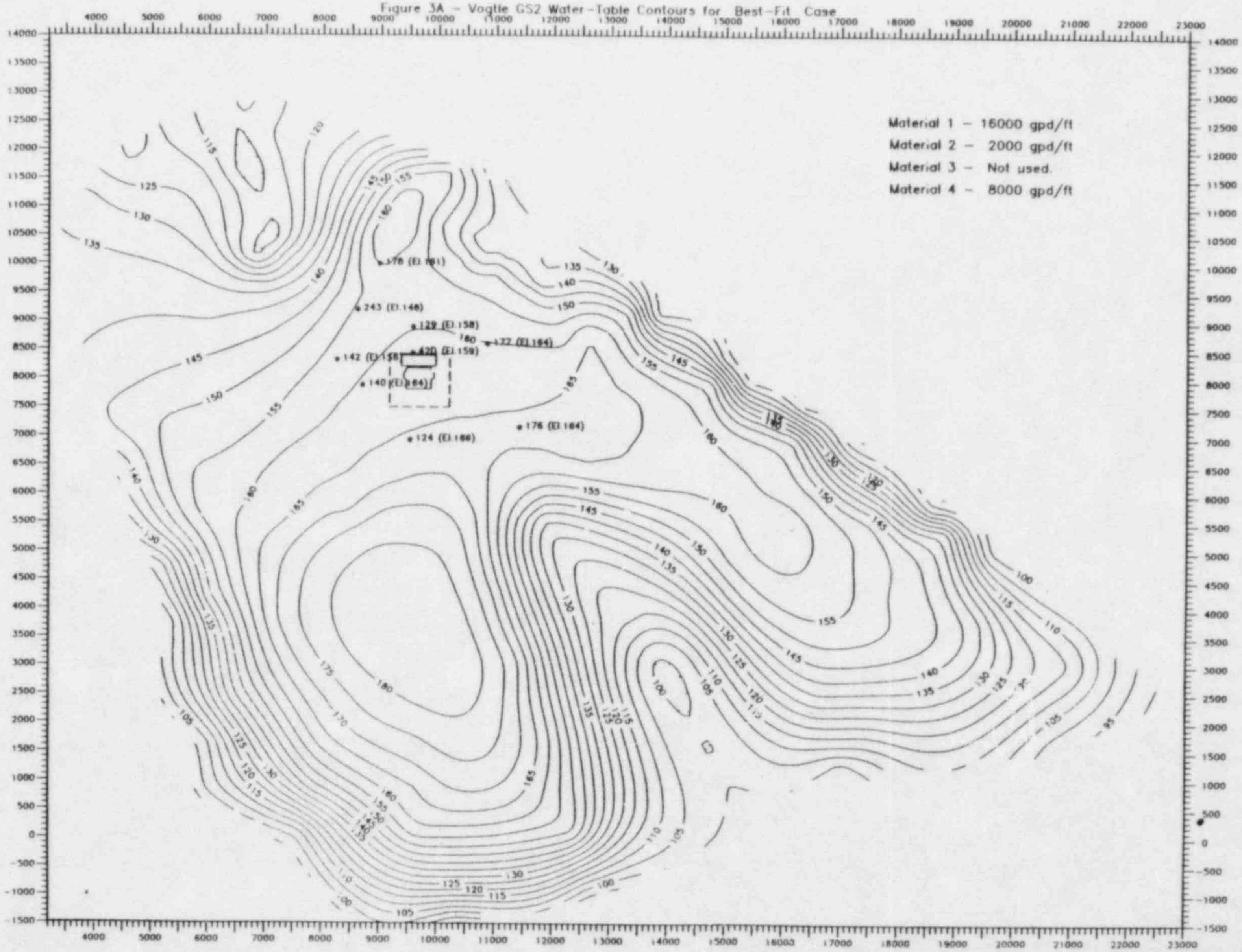

Figure 3B - Vogtle GS2 Water-Table Contours for Best-Fit Case

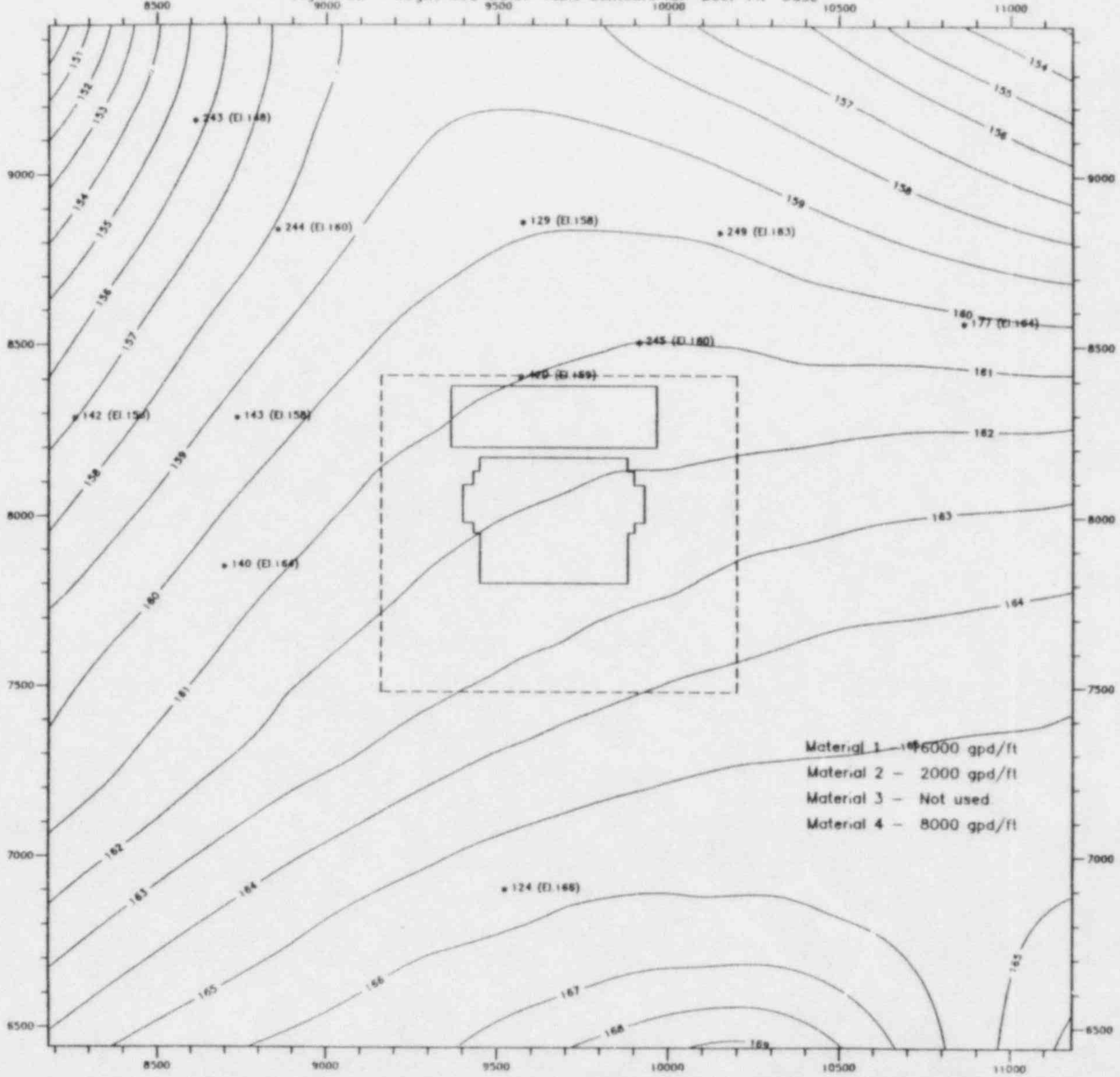

Figure 4A – Vogtle GS2 Water-Table Contours for Test Case 1

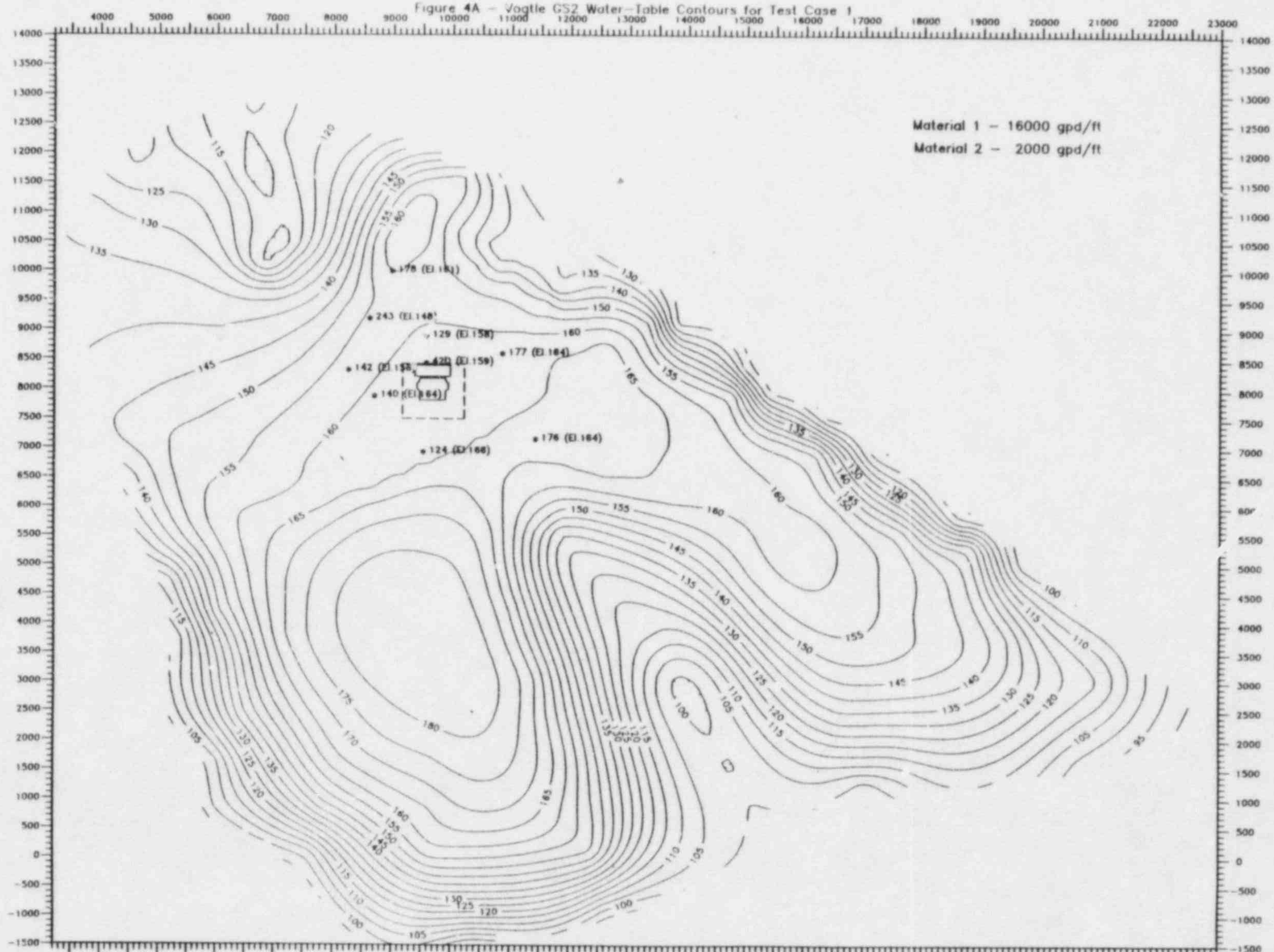

Contour Interval 5.0

Figure 4B - Vogtle GS2 Water-Table Contours for Test Case 1

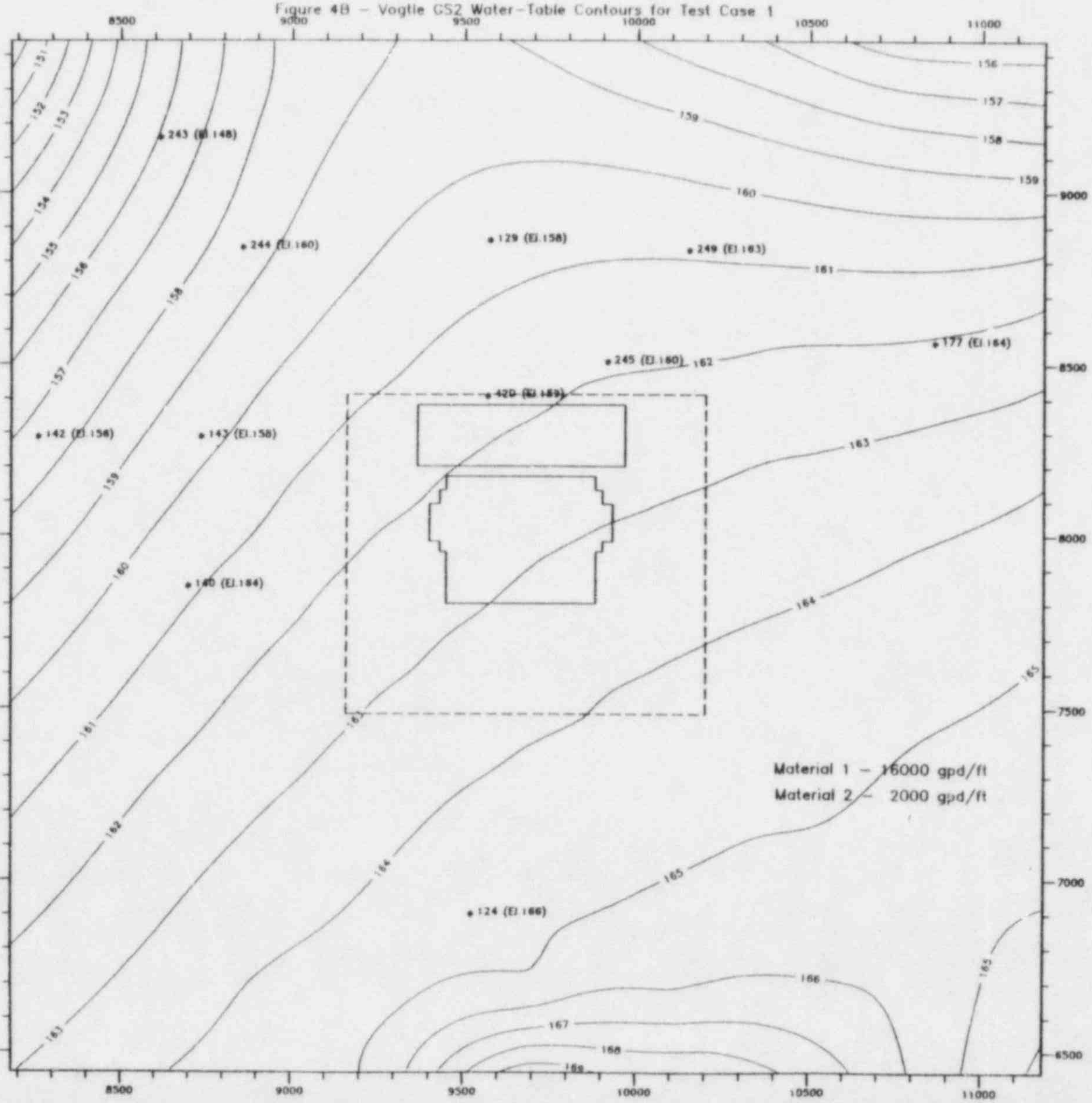

Contour Interval 1 ft

Figure 5A – Vogtle GS2 Water-Table Contours for Test Case 2

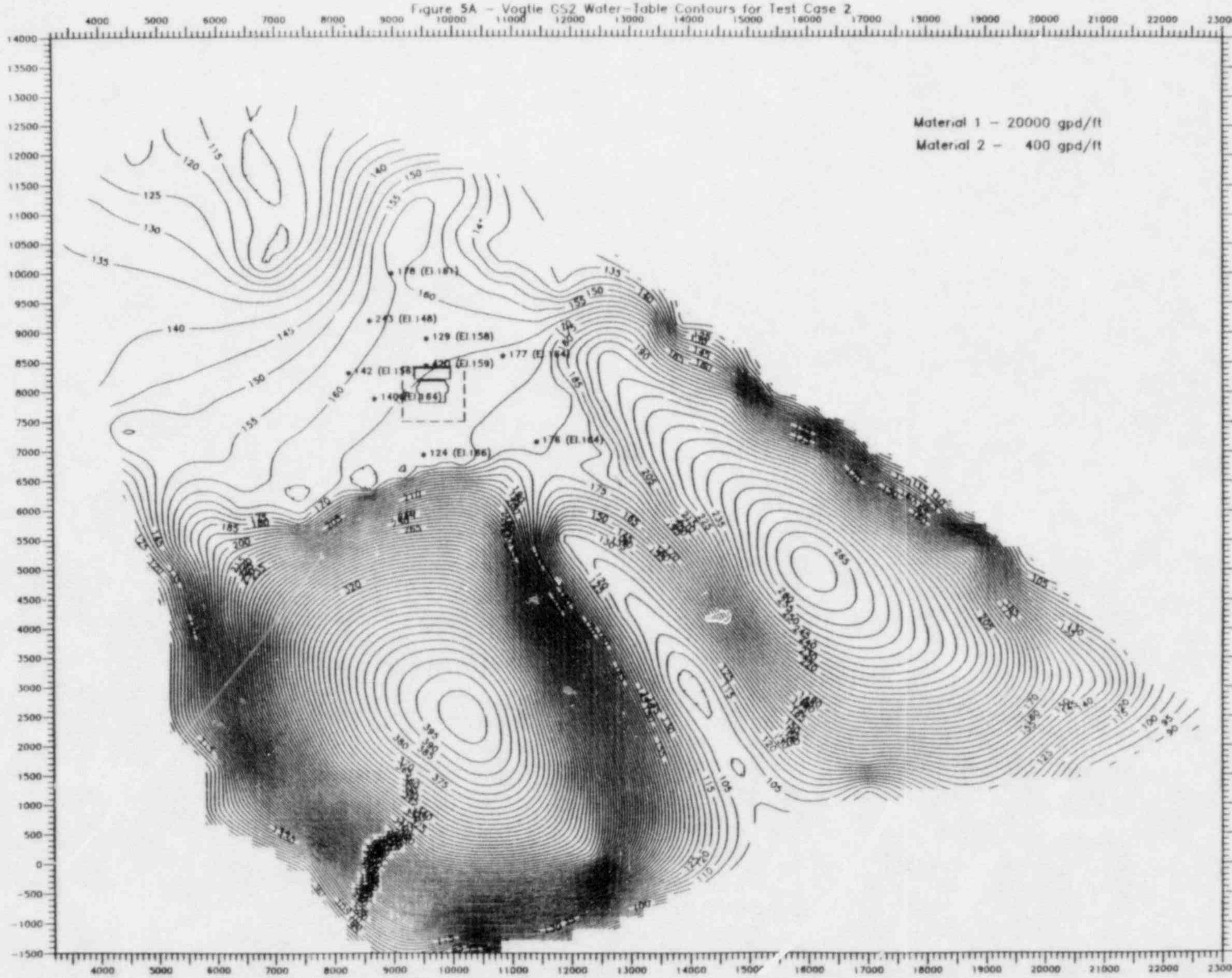

Contour Interval 5 ft

Figure 5B – Vogtle GS2 Water-Table Contours Test Case 2

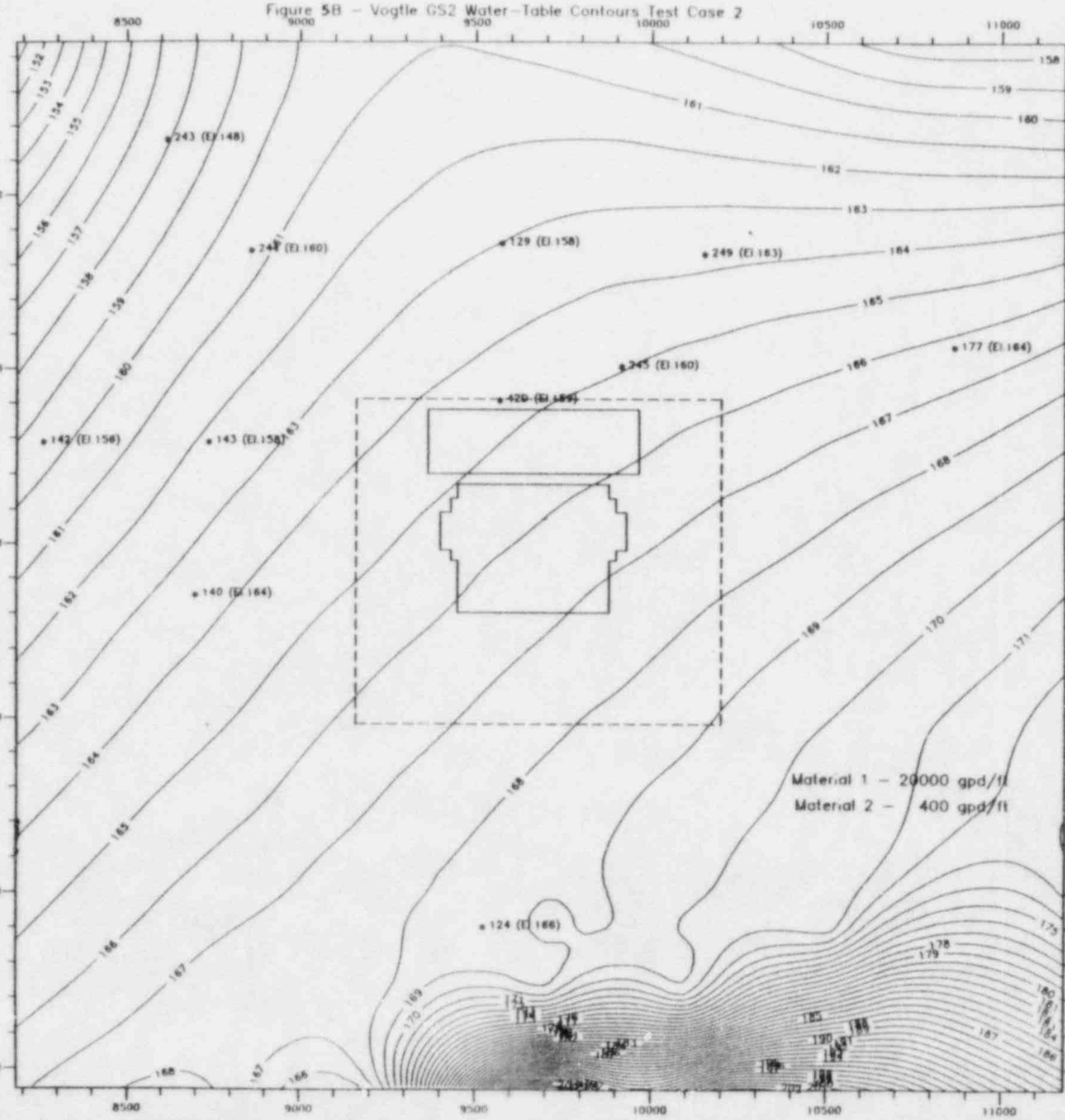

Figure 6A – Vogtle GS2 Water-Table Contours for Test Case 3

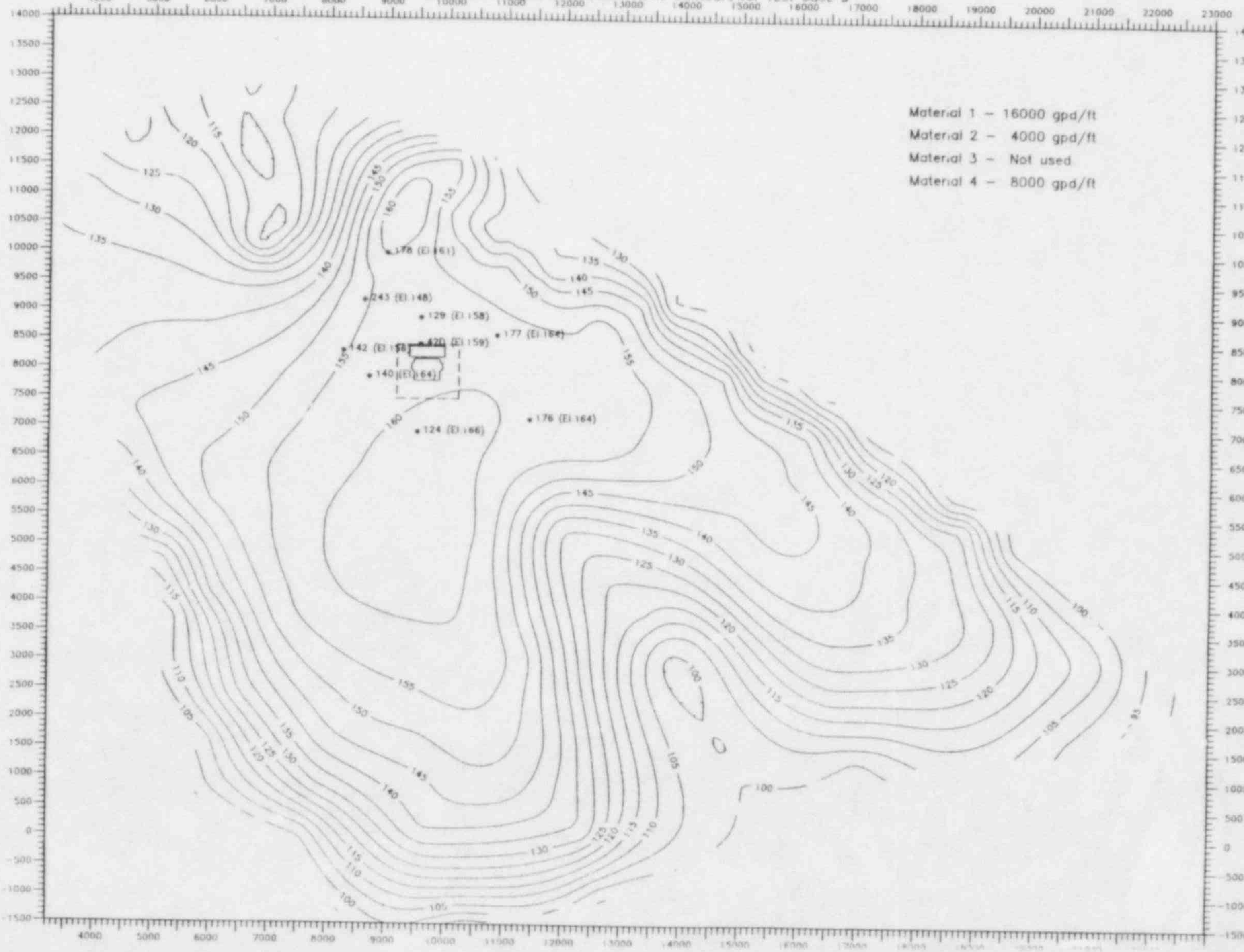

Figure 6B - Vogtle GS2 Water-Table Contours for Test Case 3

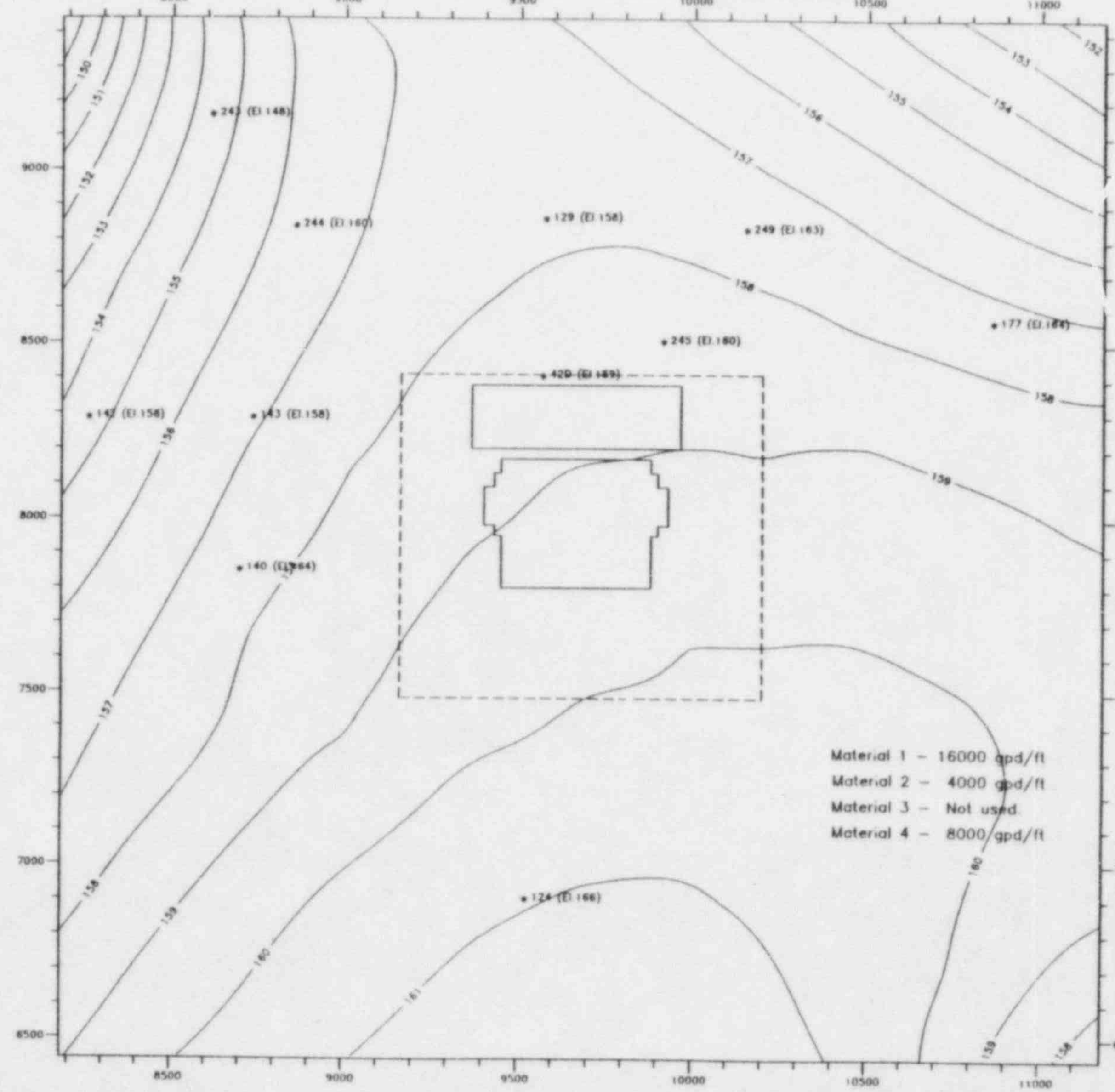

Figure 7A – Vogtle GS2 Water-Table Contours for Test Case 4

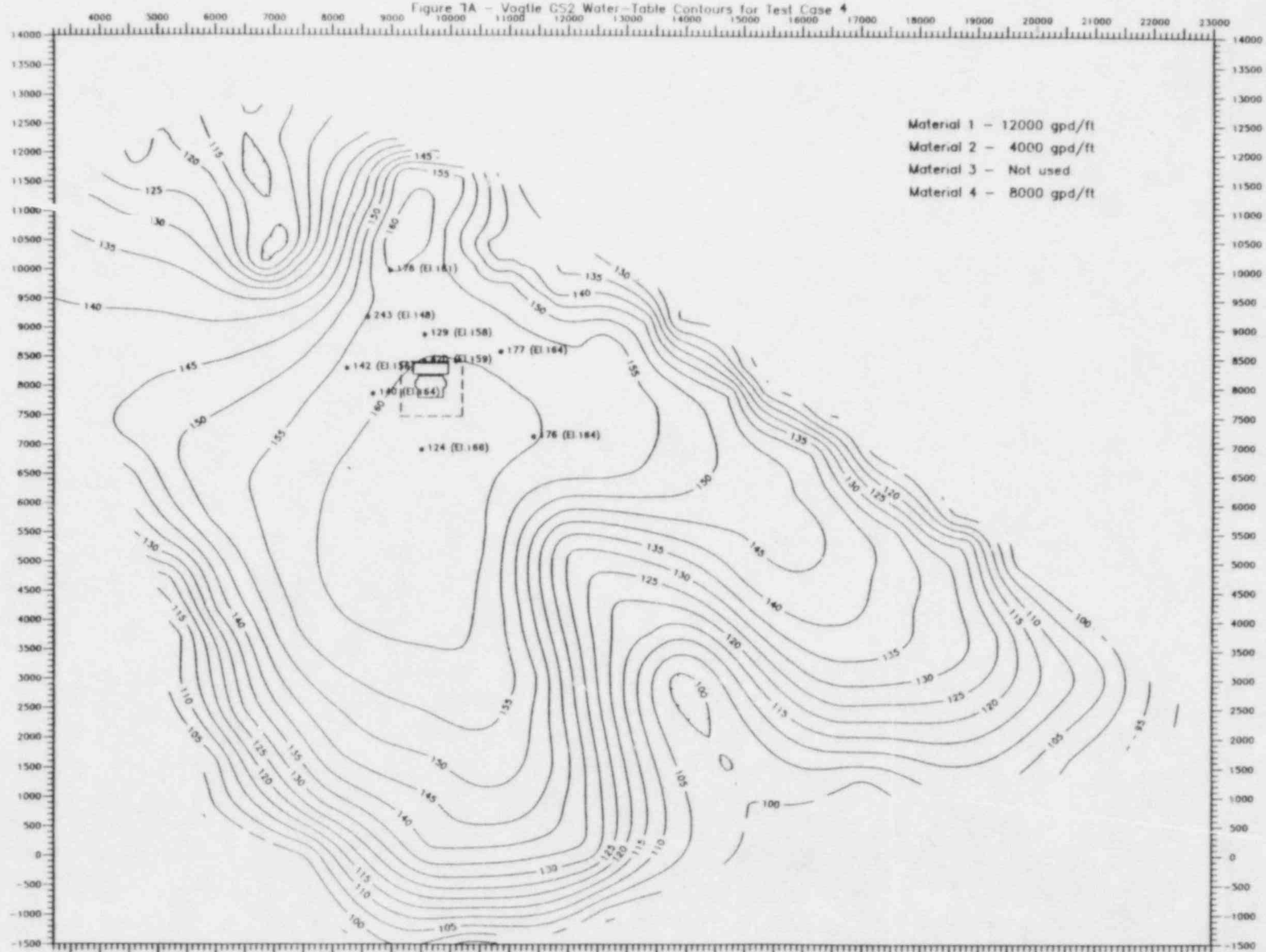

Contour Interval 5 ft

Figure 7B - Vogtle GS2 Water-Table Contours for Test Case 4

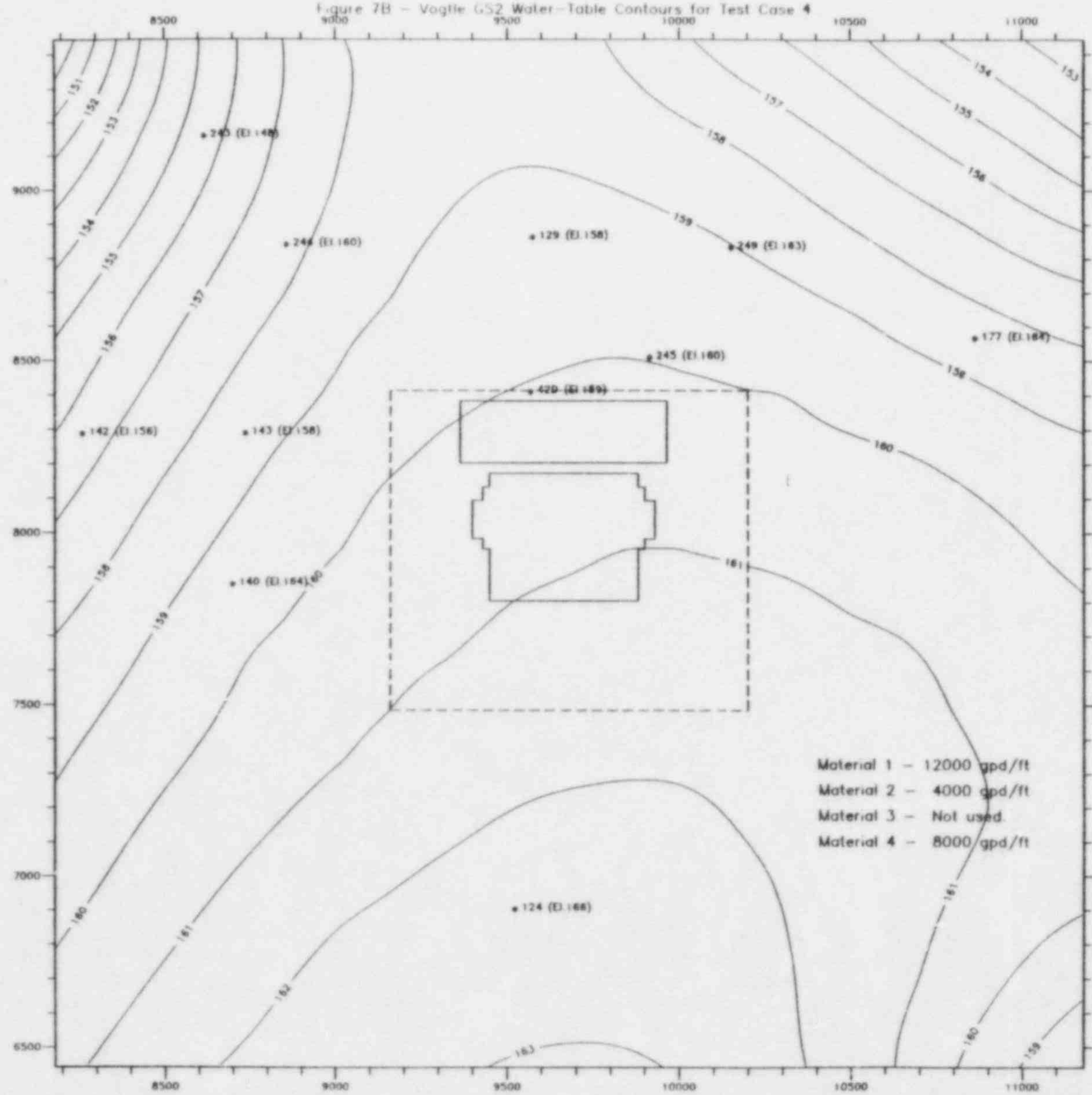

Contour Interval 1 ft

Figure 8A - Vogtle GS2 Water-Table Contours for Test Case 5

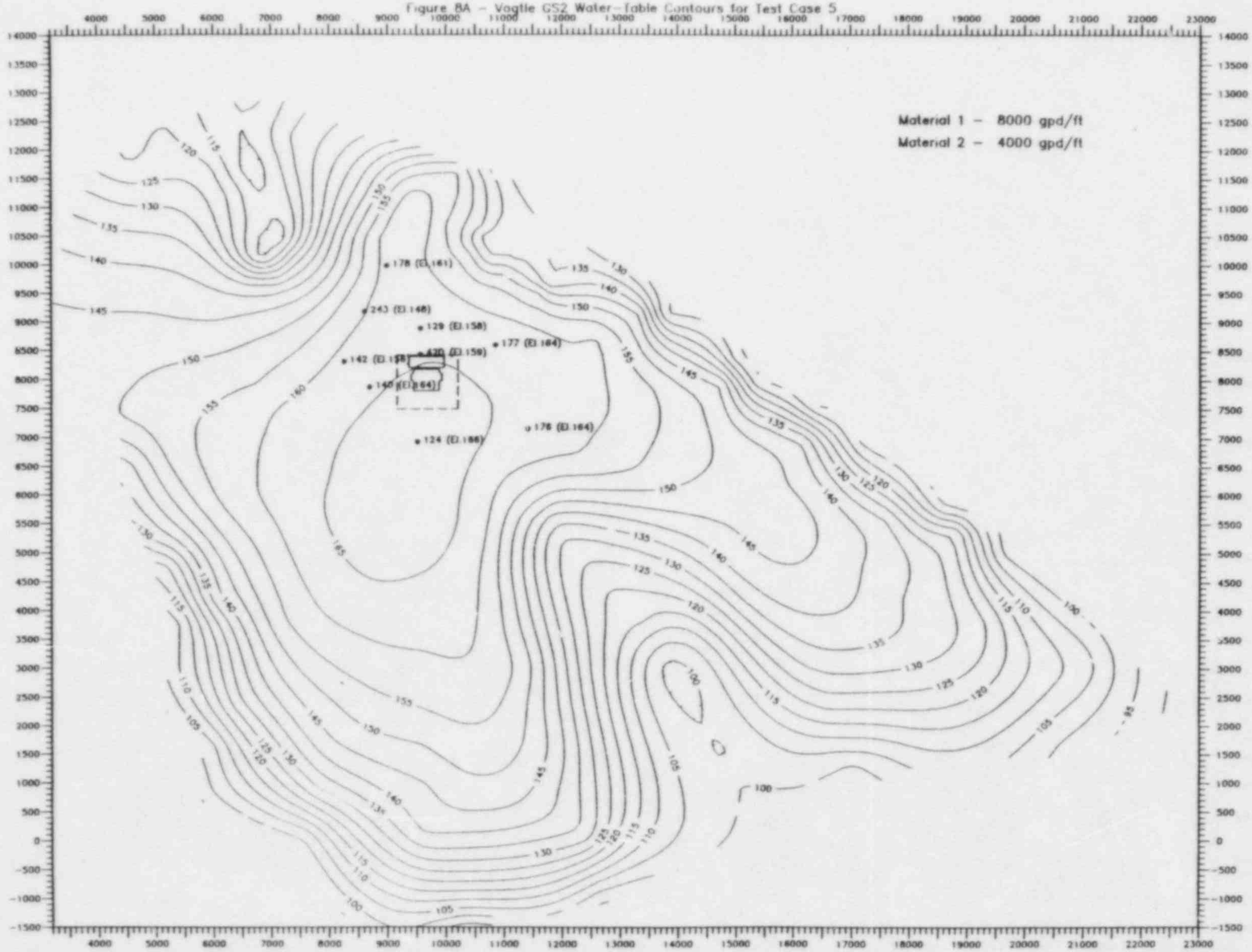

Contour Interval 5 ft

Figure 8B - Vogtle GS2 Water-Table Contours for Test Case 5

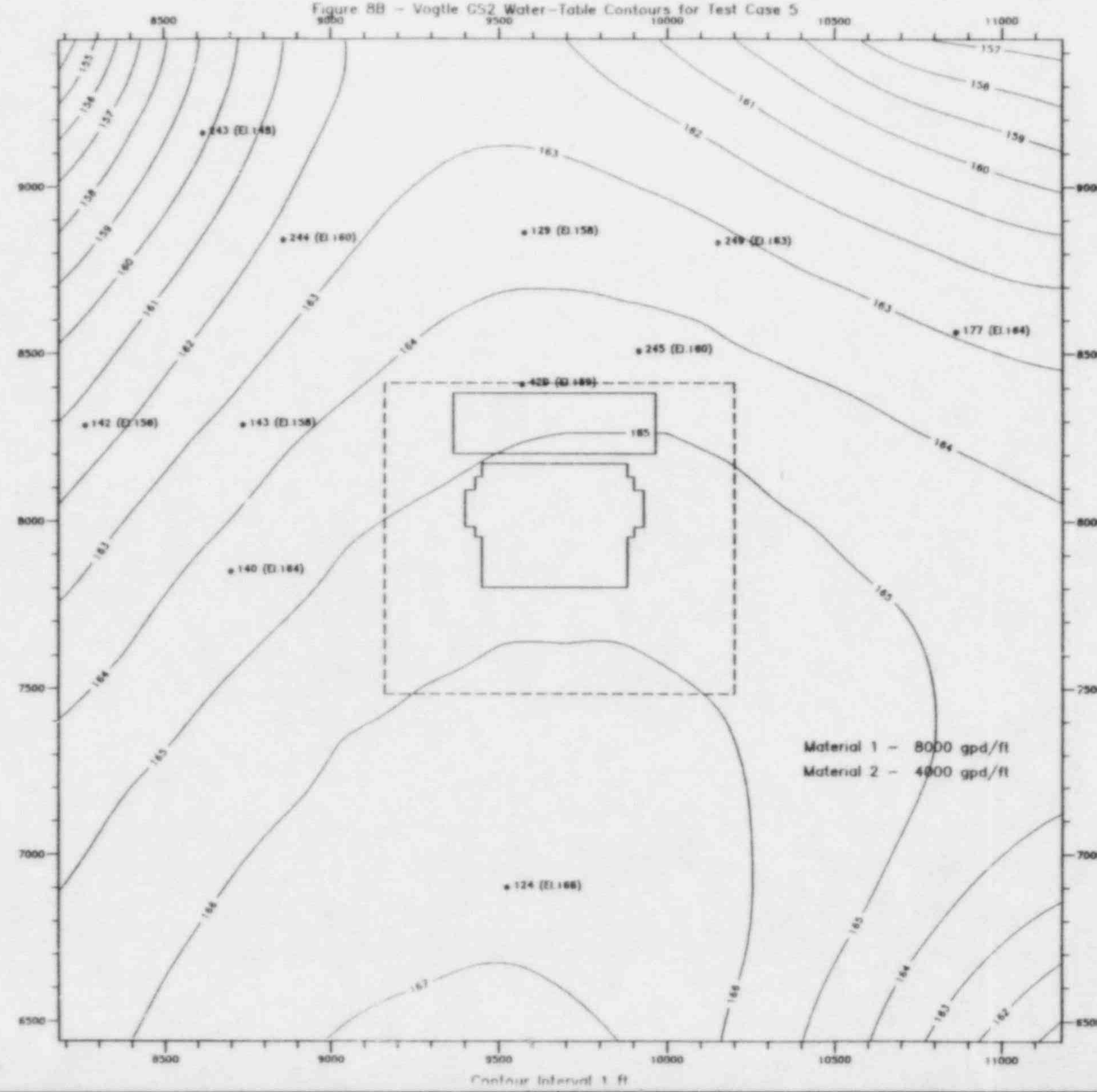

Figure 9A – Vogtle GS2 Water-Table Contours for Test Case 6

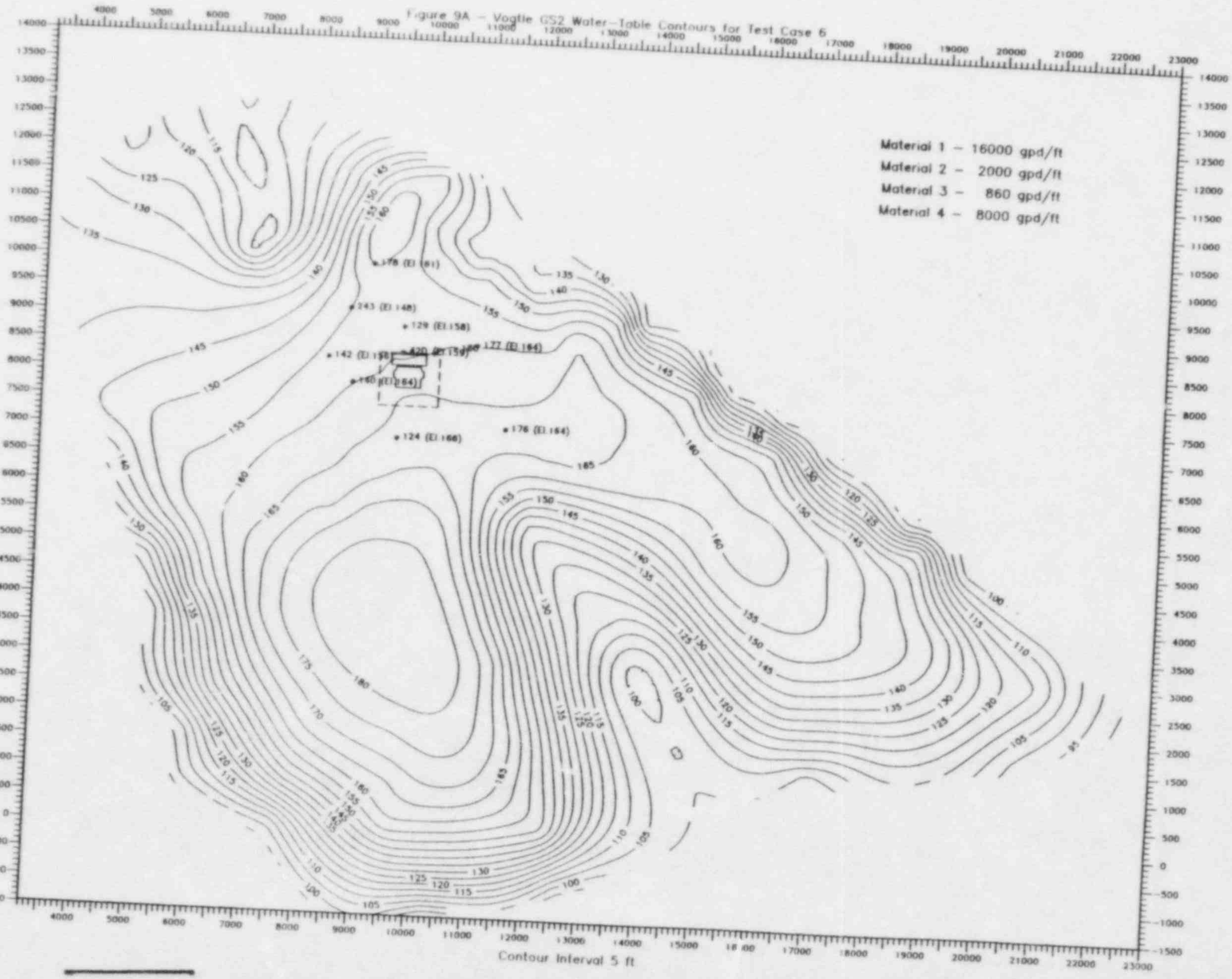

Figure 9B - Vogtle GS2 Water-Table Contours for Test Case 6